Lifetime measurements in odd-parity Rydberg series of neutral lead by time-resolved laser spectroscopy

Z. S. Li and S. Svanberg
Department of Physics, Lund Institute of Technology, P.O. Box 118, S-221 00 Lund, Sweden

E. Biémont
Institut d'Astrophysique, Université de Liège, 5 Avenue de Cointe, B-4000 Liège, Belgium

P. Palmeri
Laboratoire Aimé Cotton, Université de Paris–Sud, Bâtiment 505, F-91405 Orsay Cedex, France

Jiang Zhankui
Department of Physics, Jilin University, Chanchun 130021, People's Republic of China
(Received 11 December 1997)

Natural radiative lifetimes have been measured in the odd-parity Rydberg series $6pns$ ($n=7-13$) and $6pnd$ ($n=6-13$) of neutral lead using time-resolved UV laser-induced fluorescence from a laser-produced plasma. A relativistic Hartree-Fock calculation taking configuration interaction into account in a detailed way has also been performed for odd- as well as even-parity states for testing the ability of this approach to correctly predict radiative properties of heavy atoms. A generally good overall agreement between experimental and theoretical lifetimes has been achieved except for a few levels. [S1050-2947(98)05605-4]

PACS number(s): 32.70.Cs, 42.62.Fi

I. INTRODUCTION

In the last decade, the Rydberg states of alkali and alkaline-earth elements have been extensively investigated and their spectra have been successfully analyzed [1]. Lead is the heaviest element in the fourth group which has a p^2 ground configuration. The lowest-energy level of Pb I is $6s^2 6p^2\ (1/2,1/2)_0$, this configuration being well described by a jj coupling scheme, while the ionic core (Pb II) is $6s^2 6p$, which splits into the levels $^2P^o_{1/2}$ (lower ionization energy) and $^2P^o_{3/2}$ (upper ionization limit) in the LS coupling scheme. The Rydberg series consist of a $6p$ electron ion core and a highly excited electron, and these states are also adequately described by jj coupling.

Since the resonance lines of Pb I lie in the UV and vacuum ultraviolet (VUV) regions, only a limited amount of spectroscopic data has been obtained. Most of the work from early investigations was summarized by Moore [2]. Wood and Andrew [3] reinvestigated the Pb I emission spectrum in the spectral range 1733–39 039 Å and determined the low-lying states of odd and even parities, while Garton and Wilson [4] reanalyzed the absorption spectrum in the region 1100–2500 Å in order to study the $6pns$ ($8\leqslant n\leqslant 32$) and $6pnd$ ($6\leqslant n\leqslant 53$) states. Brown, Tilford, and Ginter [5] reported absorption observations of Pb I between 1350 and 2041 Å and analyzed the spectra in terms of the multichannel quantum defect theory (MQDT). Young, Mirza, and Duley [6], using three-photon resonance spectroscopy, investigated the even-parity Rydberg series $6pnp\ (1/2,\ 1/2)_0$ ($n\leqslant 23$), $6pnp\ (1/2,\ 3/2)_1$ ($n\leqslant 20$), $6pnp\ (1/2,\ 3/2)_2$ ($n\leqslant 48$), and $6pnf\ 1/2[5/2]_2$ ($n\leqslant 26$). Ding *et al.* [7] studied the even-parity $J=0$ and 2 Rydberg series [i.e., $6pnp\ (1/2,\ 1/2)_0$ ($n\leqslant 27$), $6pnp\ (1/2,\ 3/2)_2$ ($n\leqslant 41$), and $6pnf\ 1/2[5/2]_2$ ($n\leqslant 27$)] by means of two-photon resonance ionization spectroscopy. High-lying odd-parity levels have been considered by Buch, Nellessen, and Ertmer [8] using laser spectroscopy and their measurements were analyzed with Lu-Fano plots. Farooqi *et al.* [9] reported new data for the $J=0$, 1, and 2 even-parity levels of neutral lead using a two-step excitation technique in conjunction with a thermoionic diode detector. Considering earlier spectroscopic studies of the $6pns$, $6pnd$, and $6png$ Rydberg levels by Buch, Nellessen, and Ertmer [8], Dembczy'nski *et al.* [10] have carried out an interpretation of these levels with the aid of a linked-parameter method of level-fitting calculations in a large multiconfiguration basis. Recently, two-color resonance ionization spectroscopy of $J=0$, 1, and 2 even-parity levels [$6pnp\ (1/2,\ 1/2)_0$ ($n\leqslant 50$), $6pnp\ (1/2,\ 3/2)_1$ ($n\leqslant 27$), $6pnp\ (1/2,\ 3/2)_2$ ($n\leqslant 54$), $6p7p\ (3/2,\ 3/2)_0$, and $6pnf\ 1/2[5/2]_2$ ($n\leqslant 51$)] was applied to Pb I by Hasegawa and Suzuki [11] and the corresponding term energy values were analyzed with the MQDT technique.

In order to give more insight into the understanding of the properties of Rydberg states of Pb I, additional physical quantities, such as radiative lifetimes, are required. The Pb I spectrum has been the subject of a limited number of lifetime investigations, most of them being carried out by level-crossing spectroscopy (LCS) and, more particularly, by the Hanle-effect technique. Hanle-effect studies of the $6p7s\ (3/2,\ 1/2)^o_1$ and $6p8s\ (1/2,\ 1/2)^o_1$ states of lead were done by Saloman [12,13]. The lifetime and hyperfine structure of the $6p7s\ (1/2,\ 1/2)^o_1$ excited state have also been studied by Saloman and Happer [14] and by Novick, Perry, and Saloman [15] using the LCS method. The phase-shift technique has been applied by Cunningham and Link [16] to

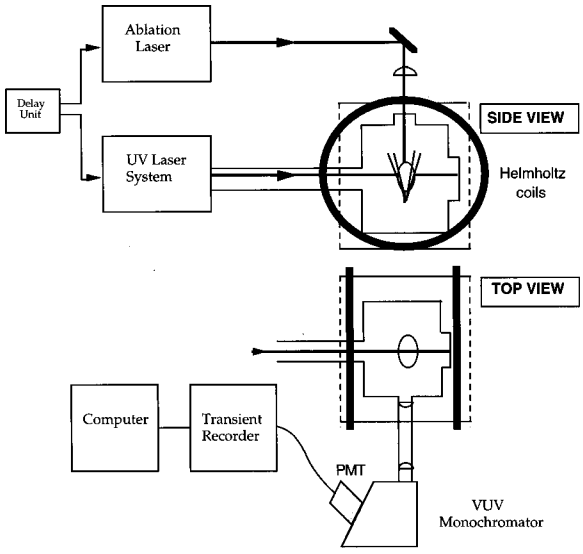

FIG. 1. Block diagram of the experimental setup.

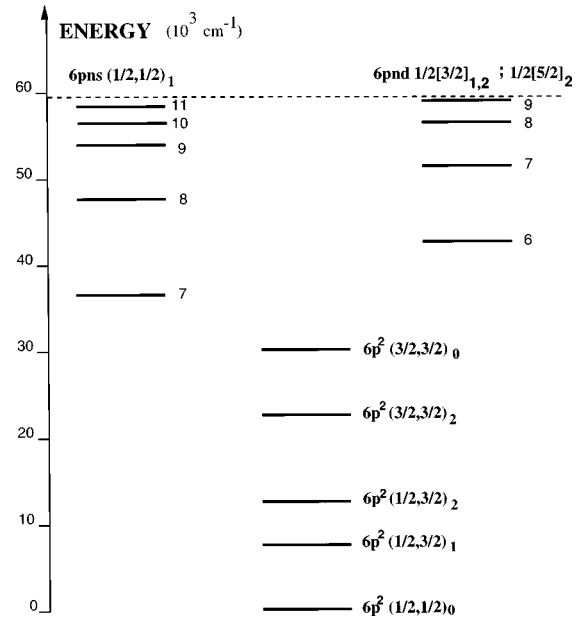

FIG. 2. Partial Grotrian diagram for odd-parity states of the neutral lead atom.

the measurement of the $6p7s\ (1/2,\ 1/2)_1^o$ lifetime value while the same level was also investigated by DeZafra and Marshall [17] by the Hanle-effect method. Garpman *et al.* [18] measured natural radiative lifetimes of some excited states of Pb I by means of the Hanle-effect method. Using optical techniques, Gibbs [19] investigated collisional quenching and depolarization of alignment of lead metastable and excited states and he was able to derive a lifetime value for the $6p7s\ (1/2,\ 1/2)_1^o$ state. The lifetimes of the $6p7s\ (3/2,\ 1/2)_1^o$ and $6p8s\ (1/2,\ 1/2)_1^o$ states of Pb I were measured by Baghdadi, Halpern, and Saloman [20] using the Hanle approach. Selective excitation of low-lying levels in neutral atoms was achieved by Ramanujam [21] by means of a fast heavy-ion-induced sputtering and this approach allowed him to measure the lifetime of the level of Pb I situated at 45 443 cm^{-1}. More recently, using the irradiation of Pb vapor by the frequency-doubled output of a nitrogen laser-pumped dye laser, the lifetime of $6p7s\ (3/2,\ 1/2)_1^o$ of atomic lead was measured by Giers, Atkinson, and Krause [22] by the observation of the excited state decay using the delayed-coincidence (DC) method. Using also the DC technique, Gorshov and Verolainen [23] were able to measure lifetimes for 12 levels ($6pns$, $n=7-8$; $6pnd$, $n=6-7$; $6pnp$, $n=8-9$) in Pb I. Beam-foil spectroscopy measurements have been reported by Andersen [24] for the $6p7s\ (1/2,\ 1/2)_1^o$ and $6p6d\ 1/2[5/2]_3^o$ levels. The hyperfine structure and isotope shift of odd-parity Rydberg states have been studied by Buch, Nellessen, and Ertmer [8] using a continuous-wave UV laser and a collimated atomic beam technique. It should be emphasized, however, that all the studies mentioned in this section were concentrated on a small number (i.e., 14) of different levels of Pb I.

Some levels along the Rydberg series of lead are strongly perturbed by configuration interaction as recently pointed out in several investigations (see, e.g., Refs. [10,11]). A detailed theoretical analysis of such effects is necessary for a better understanding of the experimental observations. Recent attempts to investigate configuration interaction in neutral lead are due to Shukla *et al.* [25], who studied the influence of valence-electron correlation effects on the fine-structure splitting in the Pb atom and the isoelectronic Bi II and Po III and to Biémont and Quinet [26] who calculated in multiconfiguration approaches the transition rates for forbidden lines within the $6p^k$ $(k=1-5)$ configurations along the lead, but also the thallium, bismuth, polonium, and actinium sequences up to radon.

For these different reasons, we report in the present paper lifetime measurements of 33 odd- and even-parity states of Pb I along Rydberg series up to $n=13$ using time-resolved laser-induced fluorescence in a laser-produced plasma. These experimental lifetime values are compared with extensive relativistic Hartree-Fock (HFR) theoretical calculations taking into account the most important relativistic effects and considering configuration interaction in a detailed way. Previously [26], this method has been shown to be adequate for providing accurate term energies and transition rates for forbidden lines in heavy atoms and ions.

II. EXPERIMENTAL SETUP

The experimental setup of the present experiment is shown in Fig. 1. The laser system used was a Nd:YAG (YAG denotes yttrium aluminum garnet) (Continuum NY-82) pumped dye laser (Continuum ND-60) operating with DCM dye or Coumarin 500 dye. To obtain the required UV radiation from 204 to 327 nm, frequency doubling and tripling of the fundamental frequency have been used. The second harmonic was produced in a potassium dihydrogen phosphate (KDP) crystal, while the third harmonic was generated by mixing the second harmonic with the remaining fundamental frequency in a BBO crystal following a retarding plate used to make the polarization direction of the second harmonic and of the fundamental frequency parallel. The excitation beam was sent through the vacuum chamber, where the atomic beam was crossed. Fluorescence light was collected with CaF_2 lenses perpendicularly to the laser and the atomic beam through amonochromator (Acton Model

TABLE I. Odd-parity levels of Pb I: levels measured and excitation scheme.

Level[a]	E_{expt}[b] (cm^{-1})	Excitation		Observed fluorescence (nm) (vac.)
		Origin	λ (nm) (vac.)	
$6p7s(3/2,\ 1/2)^o_2$	48 188.67	$6p^2(1/2,\ 3/2)_2$	266.765	247.6
$6p8s(1/2,\ 1/2)^o_1$	48 686.93	$6p^2(1/2,\ 1/2)_0$	205.394	262.9
$6p9s(1/2,\ 1/2)^o_1$	53 511.15	$6p^2(1/2,\ 1/2)_1$	218.859	188.9
$6p10s(1/2,\ 1/2)^o_1$	55 720.36	$6p^2(1/2,\ 1/2)_1$	208.765	179.5
$6p11s(1/2,\ 1/2)^o_1$	56 942.05	$6p^2(1/2,\ 1/2)_2$	216.022	175.6
$6p12s(1/2,\ 1/2)^o_1$	57 688.57	$6p^2(1/2,\ 1/2)_2$	212.594	173.3
$6p13s(1/2,\ 1/2)^o_1$	58 177.97	$6p^2(1/2,\ 1/2)_2$	210.405	171.9
$6p6d\ \ 1/2[5/2]^o_2$	45 443.17	$6p^2(1/2,\ 3/2)_1$	265.789	287.4
$6p6d\ \ 1/2[3/2]^o_2$	46 060.84	$6p^2(1/2,\ 3/2)_1$	261.494	282.4
$6p6d\ \ 1/2[3/2]^o_1$	46 068.44	$6p^2(1/2,\ 1/2)_0$	217.068	261.4
$6p6d\ \ 3/2[5/2]^o_2$	58 517.71	$6p^2(1/2,\ 3/2)_1$	208.911	197.2
$6p7d\ \ 1/2[3/2]^o_2$	52 311.32	$6p^2(3/2,\ 3/2)_2$	324.113	224.8
$6p7d\ \ 1/2[3/2]^o_1$	52 499.64	$6p^2(1/2,\ 1/2)_1$	322.147	190.5
$6p7d\ \ 1/2[5/2]^o_2$	52 101.66	$6p^2(3/2,\ 3/2)_2$	326.335	241.2
$6p8d\ \ 1/2[3/2]^o_1$	55 158.19	$6p^2(1/2,\ 1/2)_1$	211.244	181.3
$6p8d\ \ 1/2[3/2]^o_2$	55 084.14	$6p^2(1/2,\ 3/2)_1$	211.574	225.1
$6p8d\ \ 1/2[5/2]^o_2$	55 003.29	$6p^2(1/2,\ 3/2)_1$	211.937	223.5
$6p9d\ \ 1/2[3/2]^o_1$	56 604.70	$6p^2(1/2,\ 1/2)_1$	204.980	177.7
$6p9d\ \ 1/2[3/2]^o_2$	56 563.20	$6p^2(1/2,\ 3/2)_2$	217.805	205.2
$6p9d\ \ 1/2[5/2]^o_2$	56 526.49	$6p^2(1/2,\ 3/2)_2$	217.970	205.3
$6p10d\ \ 1/2[3/2]^o_1$	57 471.17	$6p^2(1/2,\ 1/2)_2$	213.581	174.0
$6p10d\ \ 1/2[3/2]^o_2$	57 444.52	$6p^2(1/2,\ 3/2)_2$	213.702	201.5
$6p10d\ \ 1/2[5/2]^o_2$	57 424.02	$6p^2(1/2,\ 3/2)_2$	213.796	201.7
$6p11d\ \ 1/2[3/2]^o_1$	58 029.94	$6p^2(1/2,\ 1/2)_2$	211.062	172.3
$6p11d\ \ 1/2[3/2]^o_2$	58 012.05	$6p^2(1/2,\ 3/2)_2$	211.142	199.2
$6p11d\ \ 1/2[5/2]^o_2$	57 995.90	$6p^2(1/2,\ 3/2)_2$	211.214	199.3
$6p12d\ \ 1/2[3/2]^o_2$	58 398.71	$6p^2(1/2,\ 3/2)_2$	209.432	199.7
$6p12d\ \ 1/2[5/2]^o_2$	58 378.56	$6p^2(1/2,\ 3/2)_2$	209.521	197.8
$6p13d\ \ 1/2[5/2]^o_2$	58 666.69	$6p^2(1/2,\ 3/2)_2$	208.262	196.7

[a]Designations according to Ref. [3].
[b]From Refs. [3, 5].

VM502) and detected by a photomultiplier tube (PMT) (Hamamatsu R1220). The data acquisition and treatment were performed by using a digital oscilloscope (Tektronix Model DSA 602) and a personal computer.

In order to populate sufficiently the metastable states in the atomic beam, a laser-produced plasma has been used. The radiation from a second Nd:YAG laser (Continuum Surelite) was focused on the surface of lead sulfide powder, about 15 mm below the excitation laser beam. A pulse energy of about 20 mJ caused ablation of the powder which was splashing at the laser pulse impact. To maintain a smooth target surface for the next laser pulse, the container was shaken by an electromagnet at a frequency in resonance with the mechanical vibrations of the container-magnet arrangement. Both Nd:YAG lasers were externally triggered by a Stanford Research Systems Model 535 digital delay generator. This allowed us to change the time delay between the light pulses used for atomization and excitation.

III. MEASUREMENTS AND RESULTS

Some energy levels of neutral lead relevant to the present experiment are shown in the partial Grotrian diagram of Fig.

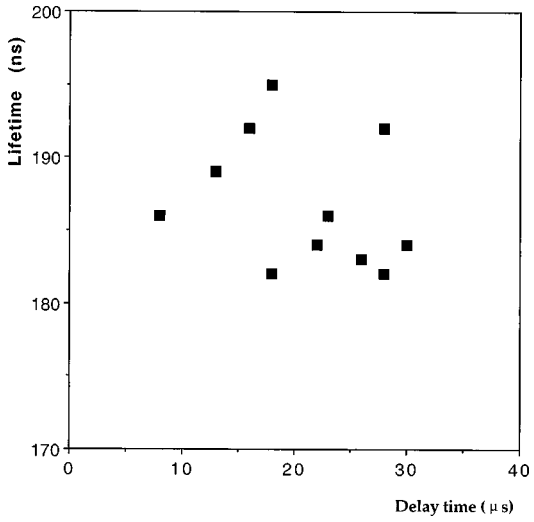

FIG. 3. Measured radiative lifetime of the $6p12s\ (1/2,\ 1/2)^o_1$ state as a function of delay time.

2. In the laser-induced plasma, all the metastable states of the configuration $6p^2$ have been sufficiently populated which allows the selection of appropriate transitions for exciting the desired levels. The transitions used in practice in the present experiment are indicated in Table I.

In order to obtain reliable lifetime values, we used time-resolved laser spectroscopy ensuring appropriate experimental conditions. A sufficiently strong magnetic field has been applied to wash out Zeeman quantum beats. To make sure that the measured lifetimes are not affected by radiation trapping or by collisional effects in the laser-produced plasma, we performed experiments with different time delays between the atomization laser pulse and the excitation laser pulse. As an example, a plot of evaluated lifetime values versus delay time is given in Fig. 3 for the $6p12s\ (1/2,\ 1/2)_1^o$ state. We found that, after a sufficiently long delay from the ablation pulse (about 8 μs), the evaluated lifetime was almost constant. A detailed discussion of the characteristics of the atomic plasma produced by laser ablation from a PbS powder surface has been given by Berzinsh *et al.* [27]. To eliminate the flight-out-of-view effect, the slit of the detection monochromator was set parallel to the ablation beam. Effects from collisions between the excited atoms and the residual gas (air) in the chamber were investigated by increasing the background pressure by an order of magnitude. The lifetimes measured in these circumstances were not found to be shorter than those obtained at the best achievable background pressure. A crucial point in a transient-recording experiment is to ensure that the detector has a linear response. In the present experiment, the number of photons recorded in each transient was small enough to exclude influence from a nonlinear effect of the detector. Four thousand shots have been accumulated for each recording to make a smooth curve. For the levels which have a lifetime longer than 10 ns, a least-squares exponential fitting of the recorded fluorescence has been used to evaluate the lifetimes. Only that part of the curves that was recorded after the turn off of the laser pulse (when the laser intensity was 0.1% of the peak value) was used in the fit. The starting point of the fit was varied to make sure that no deviations from an exponential shape of the signal influenced the measurements. The lifetimes shorter than 10 ns were evaluated by fitting a convolution of an exponential and a laser pulse as registered by the same detection system. For each state, about 30–40 curves have been recorded for different experimental conditions. The lifetime values, evaluated from the curve recorded after a sufficiently long delay from the ablation pulse, were averaged for obtaining the final lifetime values of each state. These final results are listed in Table II. Two standard deviations are quoted as error bars. Possible systematic shifts are not included in the error bars. The table also includes some data on even-parity states, that are now being studied [28].

TABLE II. Pb I: calculated and observed lifetimes and comparison with previous results.

		Lifetime value (ns)		
		This work		
Level[a]	E_{expt}[b] (cm^{-1})	Expt.	HFR	Previous
$6p7s(1/2,\ 1/2)_0^o$	34 960		7.65	7.3 ± 0.7[c]
$6p7s(1/2,\ 1/2)_1^o$	35 287		5.47	5.75 ± 0.20,[d] 6.05 ± 0.30,[e] 5.6 ± 0.3,[f] 5.58 ± 0.72,[g] 5.59 ± 0.23,[h] 6.1 ± 0.5,[c] 5.85 ± 0.20,[i] 5.6 ± 0.5[j]
$6p7s(3/2,\ 1/2)_2^o$	48 189	6.5 ± 0.3	4.97	6.6 ± 0.7,[c] 5.85 ± 0.27[h]
$6p7s(3/2,\ 1/2)_1^o$	49 440		3.37	5.6 ± 0.5,[c] 4.99 ± 0.15,[k] 4.8 ± 0.3[l]
$6p8s(1/2,\ 1/2)_1^o$	48 687	14.7 ± 0.5	15.29	14.2 ± 1.0,[c] 12.9 ± 1.4,[m] 12.6 ± 0.5[l]
$6p9s(1/2,\ 1/2)_1^o$	53 511	33.1 ± 0.8	29.69	
$6p10s(1/2,\ 1/2)_1^o$	55 720	69 ± 1	66.67	
$6p11s(1/2,\ 1/2)_1^o$	56 942	116 ± 3	120.0	
$6p12s(1/2,\ 1/2)_1^o$	57 689	185 ± 5	208.6	
$6p13s(1/2,\ 1/2)_1^o$	58 178	275 ± 15	330.4	
$6p7p(1/2,\ 1/2)_0$	44 401		52.85	
$6p8p(1/2,\ 1/2)_0$	51 786		111.8	130 ± 10[c]
$6p8p(1/2,\ 3/2)_2$	51 944		131.4	122 ± 8[c]
$6p9p(1/2,\ 1/2)_1$	54 654		583.4	449 ± 23[n]
$6p9p(1/2,\ 1/2)_0$	54 862		198.7	274 ± 12[n]
$6p9p(1/2,\ 3/2)_1$	54 928		299.8	237 ± 11[n] 250 ± 20[c]
$6p9p(1/2,\ 3/2)_2$	54 930		292.0	240 ± 10[n]
$6p10p(1/2,\ 1/2)_1$	56 339		976.0	
$6p10p(1/2,\ 1/2)_0$	56 451		325.6	
$6p10p(1/2,\ 3/2)_1$	56 475		373.7	
$6p10p(1/2,\ 3/2)_2$	56 468		405.0	
$6p11p(1/2,\ 1/2)_1$	57 318		1271.0	
$6p11p(1/2,\ 1/2)_0$	57 381		458.6	

TABLE II. (*Continued*).

Level[a]	E_{expt}[b] (cm^{-1})	Lifetime value (ns) This work Expt.	HFR	Previous
$6p11p(1/2,\ 3/2)_1$	57 430		170.5	
$6p11p(1/2,\ 3/2)_2$	57 261		181.7	
$6p6d\ \ 1/2[5/2]^o_2$	45 443	24.5±1.2	24.75	28±2,[o] 25.8±1.3[h]
$6p6d\ \ 1/2[3/2]^o_2$	46 061	4.4±0.3	3.81	5.0±0.5,[c] $4.17^{+0.49}_{-0.31}$[h]
$6p6d\ \ 1/2[3/2]^o_1$	46 068	4.1±0.4	2.43	5.2±0.5,[c] 3.74±0.28[h]
$6p6d\ \ 1/2[5/2]^o_3$	46 329		5.82	6.08±0.26,[h] 5.9±0.5[f] 6.2±0.6[c]
$6p6d\ \ 3/2[5/2]^o_2$	58 518	9.2±0.6	4.24	
$6p7d\ \ 1/2[5/2]^o_2$	52 102	53.7±1.1	66.44	
$6p7d\ \ 1/2[3/2]^o_2$	52 311	15.7±0.6	24.24	
$6p7d\ \ 1/2[3/2]^o_1$	52 500	10.2±0.9	5.97	9.8±1.2[c]
$6p8d\ \ 1/2[5/2]^o_2$	55 003	94.5±2.1	121.9	
$6p8d\ \ 1/2[3/2]^o_2$	55 084	35.4±0.9	88.02	
$6p8d\ \ 1/2[3/2]^o_1$	55 158	17.9±0.5	14.42	
$6p9d\ \ 1/2[5/2]^o_2$	56 526	169±10	195.9	
$6p9d\ \ 1/2[3/2]^o_2$	56 563	72±2	30.94	
$6p9d\ \ 1/2[3/2]^o_1$	56 605	32±1	27.63	
$6p10d\ \ 1/2[5/2]^o_2$	57 424	187±5	324.4	
$6p10d\ \ 1/2[3/2]^o_2$	57 444	105±15	94.79	
$6p10d\ \ 1/2[3/2]^o_1$	57 471	52.1±1.5	45.02	
$6p11d\ \ 1/2[5/2]^o_2$	57 996	182±18	411.4	
$6p11d\ \ 1/2[3/2]^o_2$	58 012	199±9	201.7	
$6p11d\ \ 1/2[3/2]^o_1$	58 030	73±3	63.34	
$6p12d\ \ 1/2[5/2]^o_2$	58 379	94.2±3.1	127.3	
$6p12d\ \ 1/2[3/2]^o_2$	58 399	176±16	496.1	
$6p13d\ \ 1/2[5/2]^o_2$	58 667	152±4	206.5	
$6p6f\ \ 1/2[5/2]_2$	55 360		110.1	104±8[n]

[a]Designations according to Ref. [3].
[b]From Refs. [3,5].
[c]Gorshov and Verolainen [23]—electron excitation and delayed coincidences.
[d]Saloman and Happer [14]—Hanle effect.
[e]Cunningham and Link [16]—phase shift.
[f]Andersen [24]—beam-foil spectroscopy.
[g]DeZafra and Marshall [17]—Hanle effect.
[h]Garpman *et al.* [18]—Hanle effect.
[i]Giers, Atkinson, and Krause [22]—laser excitation and delayed coincidences.
[j]Novick, Perry, and Saloman [15]—level crossing.
[k]Saloman [13]—Hanle effect.
[l]Baghdadi, Halpern, and Saloman [20]—level crossing.
[m]Saloman [12]—Hanle effect.
[n]Li *et al.* [28]—time-resolved laser spectroscopy.
[o]Ramanujam [21]—cathodic sputtering and delayed coincidences.

IV. THE CALCULATIONS

A pseudorelativistic Hartree-Fock method, originally introduced by Cowan and Griffin [29], was used for the calculations. The computer suite of programs has been described by Cowan [30]. The most important relativistic effects, such as the Darwin term and the mass-velocity contributions, were included in the calculations.

A considerable amount of configuration interaction has been explicitly introduced in the computations. The 42 configurations retained were $6s^26p^2+6s^26pnp$ $(7\leqslant n\leqslant 13)$ $+6s^26pnf$ $(5\leqslant n\leqslant 13)+6p^4+6s6p^2ns$ $(7\leqslant n\leqslant 10)$ and $6s^26pns$ $(7\leqslant n\leqslant 13)+6s^26pnd$ $(6\leqslant n\leqslant 13)+6s6p^3$ $+6s6p^2np$ $(7\leqslant n\leqslant 10)$, respectively.

In order to reduce as much as possible the discrepancies between computed and observed energy levels, the HFR technique was used in combination with a least-squares op-

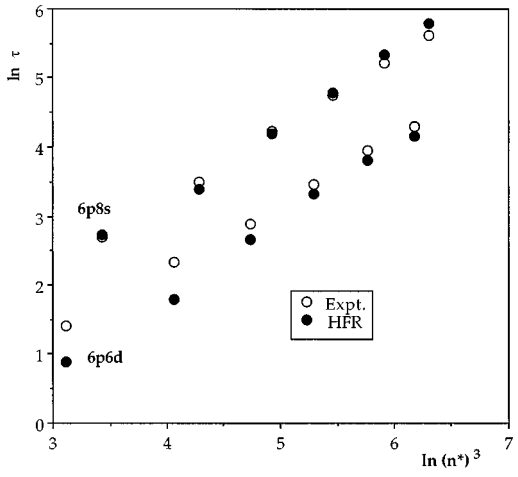

FIG. 4. Comparison of the experimental (○) and theoretical (●) lifetimes for the $6pns\ (1/2,\ 1/2)^o_1$ (upper curves) and $6pnd\ 1/2[3/2]^o_1$ (lower curves) states. $\mathrm{Log}_e\tau$ is plotted vs $\log_e[(n^*)^3]$. The straight line indicates proportionality with respect to $(n^*)^3$.

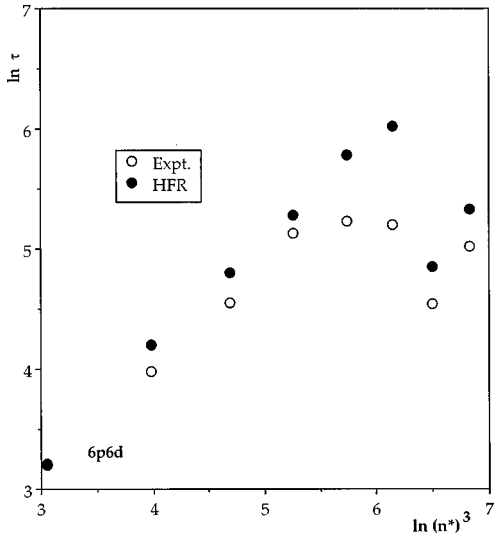

FIG. 5. Same as Fig. 4 but for the $6pnd\ 1/2[5/2]^o_2$ levels.

timization of the radial integrals according to a procedure which will be described elsewhere [31]. The parameters used in the calculations and further details about the fits will be reported there too. The experimental energy levels used for the fitting procedure were essentially taken from the spectral analyses published by Wood and Andrew [3], Brown, Tilford, and Ginter [5], and Hasegawa and Suzuki [11]. All the F^k, G^k, and R^k integrals, not optimized in the fitting procedures, were scaled down by a factor of 0.85 while the spin-orbit integrals ζ_{nl} calculated by the Blume and Watson method [32], were left at their *ab initio* values. This procedure does allow one to partly take into account interactions with configurations not introduced explicitly in the model (for a discussion, see Cowan [30]). Throughout the present work, jj coupling has been used for the level designation, even for the ground configuration, according to the analysis of Wood and Andrew [3].

The theoretical HFR lifetimes, calculated for odd- and even-parity states with the adjusted parameters, are reported in the fourth column of Table II where they are compared with the experimental results obtained in the present work (third column) and with the previously available experimental data (fifth column).

V. COMPARISON WITH PREVIOUS RESULTS AND DISCUSSION

The published experimental lifetimes for Pb I are rather scarce and concern only 14 different levels. Some of them, i.e., the $6p7s\ (1/2,\ 1/2)^o_{0,1}$, $6p7s\ (3/2,\ 1/2)^o_{1,2}$, $6p6d\ 1/2[3/2]^o_{1,2}$, and $6p6d\ 1/2[5/2]^o_{2,3}$, have been previously extensively studied. For recent discussions on lifetime measurements, see Saloman [33] and Doidge [34].

It is well established (see, e.g., [35]) that the lifetime values τ_{nl} exhibit for the Rydberg states considered in the present paper an n^{*3} scaling, n^* being the effective quantum number. Comparisons between the laser lifetime values and the HFR data, both obtained in the present work, are given in Figs. 4 and 5. In Fig. 4, both sets of results are plotted (in a logarithmic scale) vs the effective quantum number $(n^*)^3$ for the $6pns\ (1/2,\ 1/2)^o_1$ and $6pnd\ 1/2[3/2]^o_1$ series, respectively. For the first of these two series, the agreement is particularly good: the mean ratio between the theoretical and experimental lifetimes is 1.08 ± 0.07 for six levels, the quoted uncertainty representing twice the standard deviation of the mean. For the second series, i.e., $6pnd\ 1/2[3/2]^o_1$, the HFR results are systematically lower than the present laser measurements but in a consistent way: the mean ratio for six levels is 0.76 ± 0.12 and is converging to unity when n increases. For the $6pnd\ 1/2[5/2]^o_2$ Rydberg series, illustrated in Fig. 5, it is remarkable to observe that the decrease in the experimental lifetimes, which is observed for $n=12$, is adequately reproduced by theory. The behavior of the lifetime values as a function of n^* is explained by the mixing occurring between the two $6pnd\ J=2$ levels, the mixing coefficients of the $6pnd\ 1/2[3/2]^o_2$ states being found in our calculations, respectively, equal to 1.2% ($n=10$), 6.2% ($n=11$), 27.7% ($n=12$), and 11.5% ($n=13$). The larger discrepancies observed when comparing theory and experiment for $n=10$ and 11 are probably due to an underestimation of the mixing coefficients for these two states in the HFR calculation.

It should be emphasized also that, if we exclude from the mean the four levels for which the ratio $\tau_{\mathrm{theor}}/\tau_{\mathrm{expt}}$ reaches nearly a factor 2, the mean ratio for the 29 remaining levels is 1.00 ± 0.10. This overall agreement is extremely gratifying in view of the difficulties involved in the calculation of transition probabilities and radiative lifetimes in a heavy element like Pb I. In addition, the dispersion of the points does not show a dependence as a function of the energy. This satisfying agreement when comparing HFR calculations with laser lifetime measurements has been found recently in other complex situations like those met in the iron-group elements or in heavier ions (see, e.g., Biémont *et al.* [36], Pinnington *et al.* [37], and Biémont *et al.* [38]).

For the levels for which the lifetimes have not been experimentally determined in the present work, but for which data from previous experiments exist, the HFR results agree generally very well with the experiment. This is the case for the $6p7s\ (1/2,\ 1/2)_0$ level where the agreement with the

measurement of Gorshov and Verolainen [23] is within the quoted uncertainties and for $6p7s\ (1/2,\ 1/2)_1$ where the HFR result is close to most of the measurements and particularly to those of DeZafra and Marshall [17], Andersen [24], Garpman *et al.* [18], and Novick, Perry, and Saloman [15]. For $6p6d\ 1/2[3/2]_2$, theory confirms the ''low'' result obtained by Garpman *et al.* [18]. For the level $6p6d\ 1/2[5/2]_3$ at 46 329 cm^{-1}, the theoretical lifetime is in excellent agreement with the three available measurements obtained by different methods and, respectively, due to Garpman *et al.* [18], Andersen [24], and Gorshov and Verolainen [23]. For the two levels $6p8p\ (1/2,\ 1/2)_0$ and $6p8p\ (1/2,\ 3/2)_2$, the only measurements available for comparison are the DC results of Gorshov and Verolainen [23] which, again, agree well with theory confirming the general agreement observed when comparing theory with the results obtained by these authors: the mean ratio τ_{expt}/τ_{theor} is 1.16 ± 0.18, for ten levels, if we exclude from the mean the HFR lifetime value for $6p6d\ 1/2[3/2]_1$ which is obviously too short.

The excellent agreement, which is observed in the present work when comparing theoretical and experimental lifetimes in Pb I, is in favor of using a combination of laser lifetimes with HFR branching ratios for providing the astrophysicists with the accurate transition probabilities needed for specific transitions used in abundance determinations in the stars. The advantages and limitations of this procedure will be examined in detail in the near future.

ACKNOWLEDGMENTS

This work was financially supported by the Swedish Natural Science Research Council, and by the National Natural Science Foundation of China. Financial support from the Belgian National Fund for Scientific Research (FNRS) is also acknowledged.

[1] See, e.g., NIST Bibliography on Atomic Energy Levels and Transition Probabilities which is accessible through the Web (http://aeldata.nist.gov/).
[2] C. E. Moore, *Atomic Energy Levels III*, Natl. Bur. Stand. (U.S.) Circ. No. 467 (U.S. GPO, Washington, DC, 1958).
[3] D. R. Wood and K. L. Andrew, J. Opt. Soc. Am. **58**, 818 (1968).
[4] W. R. S. Garton and M. Wilson, Proc. Phys. Soc. London **87**, 841 (1966).
[5] C. M. Brown, S. G. Tilford, and M. L. Ginter, J. Opt. Soc. Am. **67**, 1240 (1977).
[6] W. A. Young, M. Y. Mirza, and W. W. Duley, J. Phys. B **13**, 3175 (1980).
[7] D. Ding, M. Jin, H. Liu, and X. Liu, J. Phys. B **22**, 1979 (1989).
[8] P. Buch, J. Nellessen, and W. Ertmer, Phys. Scr. **38**, 664 (1988).
[9] S. M. Farooqi, M. Nawaz, S. A. Bhatti, M. Ahmad, and M. A. Baig, J. Phys. B **28**, 2875 (1995).
[10] J. Dembczy'nski, E. Stachowska, M. Wilson, P. Buch, and W. Ertmer, Phys. Rev. A **49**, 745 (1994).
[11] S. Hasegawa and A. Suzuki, Phys. Rev. A **53**, 3014 (1996).
[12] E. B. Saloman, Phys. Rev. **144**, 23 (1966).
[13] E. B. Saloman, Phys. Rev. **152**, 79 (1966).
[14] E. B. Saloman and W. Happer, Phys. Rev. **144**, 7 (1966).
[15] R. Novick, B. W. Perry, and E. B. Saloman, Bull. Am. Phys. Soc. **9**, 625 (1964).
[16] P. T. Cunningham and J. K. Link, J. Opt. Soc. Am. **57**, 1000 (1967).
[17] R. L. DeZafra and A. Marshall, Phys. Rev. **170**, 28 (1968).
[18] S. Garpman, G. Lidö, S. Rydberg, and S. Svanberg, Z. Phys. **241**, 217 (1971).
[19] H. M. Gibbs, Phys. Rev. A **5**, 2408 (1972).
[20] A. Baghdadi, J. B. Halpern, and E. B. Saloman, Phys. Rev. A **7**, 403 (1973).
[21] P. S. Ramanujam, Phys. Rev. Lett. **39**, 1192 (1977).
[22] D. H. Giers, J. B. Atkinson, and L. Krause, Can. J. Phys. **62**, 1616 (1984).
[23] V. N. Gorshov and Ya. F. Verolainen, Opt. Spectrosk. **58**, 1383 (1985) [Opt. Spectrosc. **58**, 848 (1985)].
[24] T. Andersen, Nucl. Instrum. Methods **110**, 35 (1973).
[25] A. Shukla, M. Dolg, H.-J. Flad, A. Banerjee, and A. K. Mohanty, Phys. Rev. A **55**, 3433 (1997).
[26] E. Biémont and P. Quinet, Phys. Scr. **54**, 36 (1996).
[27] U. Berzinsh, L. Caiyan, R. Zerne, S. Svanberg, and E. Biémont, Phys. Rev. A **55**, 1836 (1996).
[28] Z. S. Li, U. Berzinsh, A. Persson, and S. Svanberg (unpublished).
[29] R. D. Cowan and D. C. Griffin, J. Opt. Soc. Am. **66**, 1010 (1976).
[30] R. D. Cowan, *The Theory of Atomic Structure and Spectra* (University of California Press, Berkeley, 1981).
[31] E. Biémont, Z. S. Li, and S. Svanberg (unpublished).
[32] M. Blume and R. E. Watson, Proc. R. Soc. London, Ser. A **270**, 127 (1962); **271**, 565 (1963).
[33] E. B. Saloman, Spectrochim. Acta B **45**, 37 (1990).
[34] P. S. Doidge, Spectrochim. Acta B **50**, 209 (1995).
[35] T. F. Gallagher, *Rydberg Atoms* (Cambridge University Press, Cambridge, England, 1994).
[36] E. Biémont, M. Baudoux, R. L. Kurucz, W. Ansbacher, and E. H. Pinnington, Astron. Astrophys. **249**, 539 (1991).
[37] E. H. Pinnington, G. Rieger, J. A. Kernahan, and E. Biémont, Can. J. Phys. **75**, 1 (1997).
[38] E. Biémont, E. H. Pinnington, J. A. Kernahan, and G. Rieger, J. Phys. B **30**, 2067 (1997).